HHS Public Access

Author manuscript

Biomaterials. Author manuscript; available in PMC 2016 May 01.

Published in final edited form as:

Biomaterials. 2015 May ; 51: 303–312. doi:10.1016/j.biomaterials.2015.02.025.

Capture of endothelial cells under flow using immobilized vascular endothelial growth factor

Randall J. Smith Jr.[2], **Maxwell T. Koobatian**[3], **Aref Shahini**[1], **Daniel D. Swartz**[3,4,5], and **Stelios T. Andreadis**[1,2,5,*]

[1]Department of Chemical and Biological Engineering, University at Buffalo, State University of New York, Amherst, NY 14260-4200

[2]Department of Biomedical Engineering, University at Buffalo, State University of New York, Amherst, NY 14260-4200

[3]Department of Physiology and Biophysics, University at Buffalo, State University of New York, Amherst, NY 14260-4200

[4]Department of Pediatrics, Women and Children's Hospital of Buffalo, University at Buffalo, State University of New York, Amherst, NY 14260-4200

[5]Center of Excellence in Bioinformatics and Life Sciences, University at Buffalo, State University of New York, Amherst, NY 14260-4200

Abstract

We demonstrate the ability of immobilized vascular endothelial growth factor (VEGF) to capture endothelial cells (EC) with high specificity under fluid flow. To this end, we engineered a surface consisting of heparin bound to poly-L-lysine to permit immobilization of VEGF through the C-terminal heparin-binding domain. The immobilized growth factor retained its biological activity as shown by proliferation of EC and prolonged activation of KDR signaling. Using a microfluidic device we assessed the ability to capture EC under a range of shear stresses from low (0.5 dyne/cm^2) to physiological (15 dyne/cm^2). Capture was significant for all shear stresses tested. Immobilized VEGF was highly selective for EC as evidenced by significant capture of human umbilical vein and ovine pulmonary artery EC but no capture of human dermal fibroblasts, human hair follicle derived mesenchymal stem cells, or mouse fibroblasts. Further, VEGF could capture EC from mixtures with non-EC under low and high shear conditions as well as from complex fluids like whole human blood under high shear. Our findings may have far reaching implications, as they suggest that VEGF could be used to promote endothelialization of vascular grafts or neovascularization of implanted tissues by rare but continuously circulating EC.

*Address for all Correspondence: Stelios T. Andreadis, Bioengineering Laboratory, 908 Furnas Hall, Department of Chemical and Biological Engineering University at Buffalo, State University of New York, sandread@buffalo.edu.

Keywords

VEGF; shear stress; vascular grafts; immobilized growth factor

Introduction

Coronary artery disease (CAD) is the leading cause of mortality in the United States, necessitating approximately half million coronary artery bypass graft (CABG) surgeries annually [1]. While autologous venous or arterial grafts have been the gold standard for many years, up to 30% of patients requiring venous grafts lack transplantable veins [2, 3]. Limited availability of suitable autologous vessels, morbidity at the donor site, and the high rate of long-term failure of venous grafts necessitate the search for alternative strategies [4]. Various groups have demonstrated patent tissue engineered vessels (TEVs) comprised of various biomaterial scaffolds seeded with cells in the lumen and medial layers and further preconditioned in various bioreactors exposing tissues to shear stress and/or pulsatile pressure [5–12]. Alternatively, other groups demonstrated success with scaffold-free TEV's comprised of cell sheets that were rolled and preconditioned prior to implantation and such TEVs have even progressed to human clinical trials [13–17]. However, both types of TEVs require an autologous cell source and weeks to months of culture before implantation. Consequently, development of cell-free TEVs has re-emerged recently as several laboratories demonstrated successful approaches to decellularize cell-containing TEVs and provide "off-the-shelf" transplantable grafts [18–21]. However, a functional endothelium was still necessary to maintain graft patency [22]. One group reported engineering of a completely acellular TEV that exhibited patency and remodeling in a rat animal model [23], but evidence that this approach can also work in a larger, clinically relevant animal model is still lacking. For cell-free vascular grafts, a functional lumen is necessary for successful transplantation. Methods to capture cells after implantation are emerging as an alternative strategy that aims at capturing rare circulating endothelial progenitor cells (EPCs) to repopulate the lumen and maintain graft patency.

EPCs are rare, highly proliferative, circulating cells capable of endothelializing vascular grafts, and have been a consistent target of cell capture technologies, such as microfluidic devices with appropriate surface modifications [24–27]. Of note is the capture of EPCs using surface immobilized antibodies against cell surface molecules including VEGFR2, vWF, CD31, and CD34, under low shear stress [26, 27]. In these studies cell capture occurred at shear stress lower than 4 dyne/cm^2, whereas physiological shear in arterial vessels, such as the carotids, ranges from 10–14 dyne/cm^2 [28].

While antibodies can capture cells, they may not promote and in fact, may even block cell proliferation [27]. On the other hand, growth factors are well-established inducers of cell proliferation and/or migration and may be a viable alternative to antibodies to capture rare cells. Moreover, surface immobilization of several growth factors such as NGF, EGF, GM-CSF, VEGF, and KGF has been shown to induce prolonged biological activity over their soluble counterparts [29–37]. Interestingly, the presentation of immobilized growth factors to the cells is directly related to their bioactivity and varies with the method of

immobilization [29, 38, 39]. Recently, we showed that engineered TGF-β1 fused to the fibrin binding peptide, NQEQVSP, prolonged the phosphorylation of Smad2/3 from a few hours to several days, thereby increasing deposition of collagen and elastin and improving the contractility of vascular grafts [40]. Similarly, immobilization of heparin binding growth factors such as bFGF, TGF-β2, or VEGF to heparin via their heparin-binding domain (HBD) was shown to prolong their biological activity [41–44].

VEGF is a well-known potent mitogen for endothelial cells [45–55] and a major inducer of angiogenesis - the development of new blood vessels in the body [56–62]. Binding of VEGF to heparin through the C-terminal HBD was shown to increase its biological activity, possibly by enhancing presentation of the N-terminal VEGFR binding domain [53, 63, 64] and as a result this strategy has been employed in various biomaterial applications [29, 38, 39, 65, 66]. Interestingly, VEGF bound to extracellular matrix proteins such as collagen, fibronectin, vitronectin, laminin, and matrix-associated heparin was shown to prolong VEGF receptor 2 (VEGFR2) phosphorylation and subsequent signaling events [41, 67–71]. In addition, binding of cells to matrix immobilized VEGF promoted association of VEGFR2 with β1-integrin, which in turn associated with focal adhesions, a process that did not occur with soluble VEGF [30]. Therefore, binding to heparin allows for optimal presentation of VEGF and subsequently, an enhanced cellular response.

Here we hypothesized that surface immobilized VEGF may capture endothelial cells under flow and subsequently support the proliferation and expansion of captured cells. Indeed, VEGF immobilized onto heparin could capture EC under low and high shear stress in a highly selective manner, even from complex biological fluids such as blood. Our findings suggest that this strategy may be useful in capturing rare endothelial cells for diagnostic or regenerative medicine applications.

Materials and Methods

VEGF cloning and protein production

The pGEX-VEGF plasmid was graciously provided by Dr. Te-Chung Lee of the University at Buffalo, SUNY. This plasmid encodes for a thrombin cleavable glutathione-S-transferase (GST) tag followed by the *VEGF-165* gene. For protein production, bacteria strain *E. coli* BL21-DE3-pLysis was kindly provided by Dr. Sriram Neelamegham of the University at Buffalo, SUNY. Bacteria was then expanded until O.D.=0.8, then induced with 1mM isopropyl β-D-1-thiogalactopyranoside (IPTG) for protein production for 4–6 hr at 37°C and 300rpm. The bacteria was pelleted at 20,000g for 30 min. Bacterial pellets were re-suspended in lysis buffer (50mM Tris, 500mM NaCl, 1mM ethylenediaminetetraacetic acid (EDTA), pH 8.5, 1mg/mL lysozyme, and protease inhibitors) and Triton X-100 was added at 1% prior to sonication. Sonication consisted of 10 cycles with 70% intensity, 30 s on/30 s off. Sonicated lysates were clarified by ultracentrifugation at 50,000g for 30 min. Insoluble material consisting mostly of inclusion bodies was subjected to numerous rounds of washing and sonication. The final, washed, inclusion body pellet was re-suspended in solubilization buffer (50mM Tris, 500mM NaCl, 7M Urea, 1M Guanidine-HCl, 1mM EDTA, 100mM dithiothreitol (DTT), pH of 8.5) prior to refolding by dialysis. Briefly, solubilized GST-VEGF was immediately added to a dialysis membrane (SpectraPor-1 6–8 kDa cut-off) and

dialyzed in Refolding Buffer-1 (50mM Tris, 500mM NaCl, 10mM KCl, 1mM EDTA, 2M Urea, 500mM L-Arginine, 5mM reduced glutathione, 0.5mM oxidized glutathione, pH 8.5) for 24 hr. The volume of the refolding buffer was 100× the volume of solubilized GST-VEGF. Each subsequent day the refolding buffer was replaced with half the urea concentration of the previous day for 3 days. The final dialysis step was performed in PBS. Refolding success was determined by homodimer formation as analyzed by 10% SDS-Page with and without reducing agent DTT. Properly refolded GST-VEGF has an apparent MW of 95–110 kDa, which reduces to 55 kDa upon DTT treatment. Refolded GST-VEGF was then subjected to sequential purification using GST agarose beads (Sigma, St. Lous, MO), thrombin cleavage of GST from VEGF, and a final purification step by passing cleaved VEGF through a Hitrap Heparin Column (GE Healthcare, Pittsburg, PA) according to the manufacturer's instructions.

Cell Culture

Human umbilical vein endothelial cells (HUVECs) were purchased from Lonza as a pooled donor isolation, maintained in EGM2 complete media (Lonza; Allendale, NJ) and used between passage 2 and 6 and maintained below 75% confluence. Hair follicle derived mesenchymal stem cells (HF-MSC) were isolated as described and maintained in DMEM (Life Technologies) supplemented with 10% MSC-FBS (Invitrogen) and 1ng/mL bFGF [72]. NIH-3T3 fibroblasts were purchased from American Type Culture Collection (ATCC) and maintained in DMEM supplemented with 10% BS (Invitrogen). Ovine pulmonary artery endothelial cells (OPAECs) were isolated as previously described [73] and were maintained in DMEM supplemented with 20% FBS. Human dermal fibroblasts (h-dFB) were isolated as described previously from neonatal foreskin and maintained in DMEM supplemented with 10% FBS [37]. All media supplemented with 1% Pen/Strep AA cocktail (Invitrogen). All cells were maintained in a humidified incubator with 10% CO_2 at 37°C.

Biological Activity of Recombinant VEGF

The biological activity of recombinant VEGF was assessed using a standard cell proliferation assay. To this end, HUVECs were seeded onto a 96 well plate at a density of 2×10^3 cells per well in M199 medium (Life Technologies, Grand Island, NY) supplemented with 2% heat inactivated FBS and varying concentrations of recombinant VEGF or commercial VEGF (Cell Signaling) that was used as control. Concentrations ranged from 0.05ng/ml to 100ng/ml. Cells were allowed to proliferate for 72 hr prior to treatment with 3-(4, 5-dimethylthiazol-2-yl)-2, 5-diphenyltetrazolium bromide (MTT; Life Technologies) for 4 hr. Then, the medium was carefully removed and replaced with 100 μl of DMSO to solubilize the purple formazan crystals. Absorbance was read at 570nm using a Biotek Synergy 4 Spectrophotometer (with background absorbance at 650nm subtracted).

Immobilization of VEGF

Poly-L-Lysine, MW 75,000–150,000 (Sigma) was used at the manufacturer's recommended concentration of 0.05mg/mL to coat tissue culture treated polystyrene surfaces (TC). Coating was performed by adding sterile PLL solution for 2 hr with rocking at RT. After coating with PLL, the surface was washed repeatedly with sterile water to remove unbound PLL. Heparin (17–19 kDa) from porcine submucosa (Sigma) was dissolved in sterile water

at a concentration of 5mg/mL and then applied directly to the PLL treated surfaces overnight at RT. Then the surface was washed with sterile water to remove unbound heparin and heparin binding to PLL was determined using the toluidine blue binding assay as described previously [74]. Heparin concentration on the surface was determined by comparing the unbound heparin concentration remaining in solution to the initial concentration. Briefly, unbound heparin was added to toluidine blue buffer (0.1mg toluidine blue dissolved in 50mM TBS buffer, pH 4.5) at a ratio of 1 volume toluidine blue to 12 volumes heparin. The reaction proceeded for 30 min prior to centrifugation and absorbance was measured at 631nm using a Biotek Synergy 4 Spectrophotometer (background absorbance of an empty well was subtracted from each value).

Finally, recombinant VEGF was then added to the PLL-Heparin surface. Binding of VEGF was optimal at 37°C without rocking, for 2 hr. VEGF binding was determined by ELISA using biotin-conjugated goat anti-VEGF antibody (100ng/mL, 2 hr, RT, R&D Systems), followed by incubation with streptavidin-HRP (1:200, 30 min, RT) and addition of substrate (TMB, Sigma). Absorbance was read at 450nm using a Biotek Synergy 4 Spectrophotometer (with subtraction of background absorbance of 570nm).

Static Capture of Endothelial Cells

Wells of a 48-well plate were prepared as discussed above with varying concentrations of VEGF on PLL-Heparin surfaces. All surfaces were blocked with 1% BSA for 1 hr prior to seeding. HUVECs (under 70% confluent) were removed from tissue culture plates by treatment with 5mM EDTA (10min), re-suspended in M199 medium without serum and plated at a density of 5×10^3 cells per well (7×10^3 cells/cm^2). Cells were allowed to bind to the surface for 30 min under standard culture conditions and then washed with PBS and fixed with 4% para-formaldehyde. Cells were stained with DAPI and imaged with a Zeiss *Axio O*bserver.Z1 fluorescence microscope (LSM 510; Zeiss, Oberkochen, Germany) equipped with a digital camera (ORCA-ER C4742-80; Hamamatsu, Bridgewater, NJ). Cells were counted under a 20× objective in 10 fields of view per well.

Proliferation on VEGF Functionalized Surface

To determine cell proliferation, HUVECs (under 70% confluent) were removed from tissue culture plates by treatment with 5mM EDTA (10min), re-suspended in basal EBM2 medium with 10% serum and plated at 5×10^3 cells per well on VEGF-functionalized 48-well plates with varying concentrations of VEGF. The cells were allowed to bind for 6 hr and then unbound cells were removed and the medium was changed to M199 supplemented with 2% heat inactivated FBS. After 120 hr, cells were subjected to MTT assay as described above.

Capture of cells under flow in a microfluidic device

Capture of endothelial cells under flow was assessed in a microfluidic device (Fig. 3A). The device with channel dimensions of 400μm in width, 200μm in height, and 1cm in length, contains four circular ports used for vacuum sealing to a flat surface. Functionalization of the surface with PLL and heparin, was performed as described above and using 50μg/mL VEGF to obtain complete saturation of the PLL-Heparin surface in the microchannel. The PDMS based device was washed vigorously with 100% ethanol and dried under a stream of

air before it was placed onto the functionalized surface. The input port was connected to a reservoir for media and cells, and the output port was connected to a Harvard Apparatus Syringe Pump through a Hamilton glass syringe (1 mL). The pump controlled the flow rate and therefore, the shear stress on the bottom surface of the micro channel, τ_w, in the device could be calculated according to the equation:

$$\tau_w = \frac{6\mu Q}{h^2 w_1}$$

where, μ is the viscosity; Q the volumetric flow rate; h, the height; and w_1, the width of the micro channel. DMEM without serum was used during fluidic runs with a viscosity of 0.88cP [75]. Simulation of fluid velocity through the channel in 2D is represented in Fig. 3E, but for simplicity, the formula above was used to adjust shear within the channel. All cells (under 70% confluent) were removed from tissue culture plates by treatment with 5mM EDTA (10min) and re-suspended in DMEM medium without serum at the required concentration prior to running on the device. When indicated cells were pre-stained with fluorescent carbocyanines, DIO or DIL (Life Technologies) according to manufacturer specifications to enable live cell tracking.

Acquisition of Whole Blood

Whole blood was acquired from healthy donors as per University at Buffalo IRB/IACUC guidelines and federal regulations. Whole blood was acquired using traditional methods of needle and syringe and supplemented with a tenth of acquired volume with sodium citrate and used within 4 hr.

Statistics

All experiments were performed in triplicates or higher as noted to obtain statistical significance. Statistical significance was assessed by a two-tailed student t-test and the data was considered statistically different when $p<0.05$.

Results

VEGF-165 was produced in *Escherichia coli*. as a recombinant GST tagged protein. As described above, VEGF expression was induced with IPTG and the protein was harvested as insoluble inclusion bodies followed by dialysis refolding and downstream purification (Fig. S1). Typical yields ranged from 5–10 mg/L culture. Biological activity was determined to match that of commercially available VEGF-165 via HUVEC proliferation assay, with an *ED-50* of ~ 5 ng/mL (Fig. S1D).

To immobilize VEGF in a bioactive form, tissue culture treated surfaces were first treated with poly-L-lysine (PLL) followed by heparin to utilize the heparin binding domain (HBD) of VEGF-165 (Fig. 1A). PLL has been shown to bind heparin with high affinity due to the high electrostatic interactions of the two molecules [76]. A toluidne blue binding assay was employed to measure the heparin concentration, which reached 0.763±0.05μg/cm^2 (Fig. 1B). Heparin bound to the surface only in the presence of PLL and did not bind on tissue culture

treated surfaces alone (Fig. 1B). VEGF was then immobilized only to P+H (PLL-heparin) surfaces as confirmed by ELISA. Further, using ELISA we determined the surface concentration of VEGF, which followed a sigmoidal pattern as a function of the concentration of input VEGF (Fig. 1D). In the range of VEGF concentration between 1,000 and 10,000ng/mL, approximatelty ~64%±7% of VEGF was immobilized and the surface concentration at saturation was 1,010±9.8ng/cm^2.

To assess the biological activity of immobilized VEGF, we measured proliferation of HUVEC on varying concentrations of immobilized VEGF, using the MTT assay. As shown in Fig. 2A, HUVEC proliferation increased as a function of VEGF surface concentration. Next we examined whether binding of cells to immobilized VEGF activated VEGF receptor (VEGFR) signaling. Here we focused on VEGFR2/Flk-1, the major transducer of VEGF signals in EC [77]. To this end, HUVEC were seeded onto P+H+V (PLL-Heparin-VEGF) surfaces and at the indicated times, non-adherent cells were removed and adherent cells were lysed for protein isolation. First, WB showed that VEGFR2 was phosphorylated quickly after cell binding to the surface (Fig. 2C). Phosphorylation levels were prolonged over a 90 min time period with a maximum response at 10 min. As expected, phosphorylation of the downstream kinase Erk1/2 followed VEGFR2 phosphorylation and was sustained for 30min. Such prolonged phosphorylation has also been observed when VEGF was bound to fibronectin and collagen indicating differential signaling response when bound to extracellular matrix components [30, 41, 70].

Capture of EC on VEGF functionalized surface

First we examined cell binding as a function of immobilized VEGF concentration. To this end, HUVEC were exposed to functionalized surfaces with varying VEGF concentrations in the absence of serum. After 30 min the unbound cells were washed and bound cells were counted. As shown in Fig. 2B the number of captured cells increased with increasing surface concentration of VEGF and reached a maximum between 700–1,000ng/cm^2 of VEGF.

Next, a microfluidic device was employed to assess whether immobilized VEGF could capture cells under flow (Fig. 3A). The setup of the device, microscope, and syringe pump is depicted in Fig. 3A and the flow rates with the corresponding values of shear stresses are shown in Fig. 3B. The surface of microfluidic channel was functionalized with VEGF to allow HUVEC capture as shown in Fig. 3D.

First, we evaluated the capture of HUVEC at varying shear stresses between 0.5 to 15 dyne/cm^2. Representative images of the empty channel as well as cells captured at 0.5 dyne/cm^2 are shown in Fig. 4A. At low shear, cells were captured with high efficiency and began to spread within 20 min. Increasing shear decreased the capture efficiency in a dose dependent way from 771±102 cells/mm^2 to 37±2 cells/mm^2 ($n=3–10$, $p<0.05$) (Fig. 4B). However, even the lowest capture efficiency on VEGF surfaces at 15 dyne/cm^2 was significantly higher than that of P+H control surfaces under static conditions (10±4 cells/mm^2, $n=10$, $p<0.05$).

Capture on immobilized VEGF requires active VEGF receptor pathway

Next we tested other cells types to examine whether VEGF-mediated capture was specific to endothelial cells (Fig. 5A). These experiments were performed under low shear conditions where the capture efficiency was maximum. Specifically, HUVEC were compared to ovine pulmonary artery endothelial cells (OPAEC) and three non-endothelial cell types namely, human hair follicle mesenchymal stem cells (hHF-MSC), human dermal fibroblasts (h-dFB) and a mouse fibroblast cell line (NIH-3T3). OPAEC exhibited similar capture efficiency on P+H+V as HUVEC (139±15 cells/mm^2, n=3, $p<0.05$). In contrast, neither hHF-MSC, h-dFB, nor NIH-3T3 cells bound to VEGF surfaces at a rate that was statistically significant as compared to P+H control surfaces. Taken together, these results suggest that VEGF mediated capture is specific to cells expressing VEGF receptors.

To address this hypothesis, HUVEC were first pretreated with SU5416, a well-known and potent tyrosine kinase inhibitor of VEGFR2 function [78]. Interestingly, SU5416 pretreatment prevented capture of HUVEC on P+H+V (Fig. 5B), indicating that an active VEGF pathway was required for successful cell binding and capture.

Immobilized VEGF can capture EC in complex cell mixtures under low and high shear stress

Next we examined whether immobilized VEGF can capture EC in complex cell mixtures, especially when EC represent a small fraction of the total cell population. To this end, we tested varying ratios of EC to non-EC under low shear (0.5 dyne/cm^2). HUVECs and NIH-3T3 were prepared as described for fluidic runs and diluted as needed to produce a 0:1, 1:0, 1:1, 1:10, and 1:100 ratio of HUVECs to NIH-3T3s, keeping the total cell concentration constant (1×10^4 cells per run in 100μL). As shown in Fig. 6A, the number of captured HUVEC increased linearly with the initial HUVEC cell number (solid line), whereas NIH-3T3 capture remained below control conditions (dashed line), indicating that capture was dependent on EC concentration and unaffected by the presence of other cell types.

Next we tested the low cell ratio (HUVEC:NIH-3T3 at 1:100) at intermediate (5 dyne/cm^2) and high shear stress (10 dyne/cm^2) that more closely mimic the physiological shear of the arterial circulation. For these experiments, the concentration of HUVECs was held constant at 1×10^4 cells/mL and NIH-3T3 at 9.9×10^5 cells/mL and the volume was adjusted accordingly to allow for a standard running time of 45min for both shear stresses assessed. As shown in Fig. 6B, 0.8±0.05% and 0.9±0.03% of HUVEC's were captured under 5 and 10 dyne/cm^2 respectively, (n=10, $p<0.05$ compared to control of P+H surface, 0.003±0.001% and 0.002±0.001% respectively). NIH-3T3 capture was very low and not significantly above control conditions (0.0015% and 0.0019% for 5 and 10 dyne/cm^2, respectively, n=10, $p>0.05$).

Finally, we spiked blood samples with HUVEC to test selectivity of HUVEC binding on immobilized VEGF under physiological conditions. To this end, HUVEC were pre-labeled with DIL and 5×10^3 HUVEC were mixed with 1mL of freshly drawn human blood containing approximately $5–10\times10^9$ cells per mL, yielding a ratio of HUVEC:blood cells of $1:1\times10^6$. As shown in Fig. 6C, 0.7±0.05% of HUVECs (35±5 of 5×10^3 cells per run) were

captured on P+H+V surface under high shear (10 dyne/cm^2) (n=3, $p<0.05$, as compared to the control surface).

Discussion

Repopulating vascular grafts with endothelial cells *in-vivo* is the basis for many attempts to engineer cell-free vascular grafts. Target cells usually include the rare endothelial progenitor cell (EPC), a highly proliferative cell type, with the potential to endothelialize blood vessels within the body [79]. However, the timely capture of such cells and their subsequent proliferation and maturation *in-vivo* so as to maintain patency is an ongoing challenge. Current devices utilize a wide range of techniques such as device geometry, micro-pillars, and antibodies to capture rare cells, such as EPCs, as reviewed recently [24]. However, to date, no study has identified a method to capture cells under flow and further promote the growth and differentiation of captured cells as would be required for the endothelialization of a vascular graft. Thus the purpose of this study was to investigate whether VEGF, a potent EC growth factor, could capture cells under flow and subsequently induce proliferation of the captured cells.

While previous studies showed that antibodies such as anti-CD34, -CD31, or -VEGFR2 could be used to capture cells [26, 27], surface immobilized growth factors have not been investigated in this context. This is important, as antibodies do not support cell proliferation and in many cases they block the intended action of the receptor or surface molecule. Indeed, one study showed a dose dependent decrease in proliferation of cells captured using an anti-VEGFR2 antibody [27]. On the other hand, we found that immobilized VEGF increased proliferation of captured EC in a dose dependent manner, demonstrating that in addition to capturing cells, VEGF-mediated signaling stimulated biological activity.

This finding is in agreement with previous studies that showed enhanced cellular response by immobilized growth factors. For example, immobilization of EGF or bFGF in polyethylene glycol (PEG)-based scaffolds maintained their mitogenic activity, promoted cell migration, and induced cell alignment in the direction of increased growth factor concentration [80–82]. Tethering TGF-β1 to PEG scaffolds resulted in significant increase in matrix production from fibroblasts over the same amount of soluble TGF-β1 [33]. Our laboratory recently showed that immobilization of TGF-β1 into fibrin hydrogels led to prolonged phosphorylation of Smad2, which was accompanied by increased expression of smooth muscle genes and vascular contractility [40]. Interestingly, immobilized SDF1α was successful in regenerating a cell-free vascular graft with a complete endothelium by 3 months in a small animal model [83]. However, in a more clinically relevant ovine model, SDF1α loaded grafts resulted in neointimal hyperplasia, thrombi formation in the middle of the graft, and incomplete endothelium coverage at 3 months post-implantation [84], suggesting a need for an alternative. Based on these studies, we hypothesized that immobilized VEGF may provide an efficient means of capturing EC under flow and promoting biological activity.

Indeed, our findings show that VEGF captured endothelial cells even at the highest shear stress tested (15 dyne/cm^2). As expected, the rate of cell capture decreased with increasing

shear stress but remained statistically significant as compared to control surfaces (without VEGF). It is important to note that previous studies using anti-VEGFR2, CD31, and CD34 demonstrated cell capture only up to 4 dyne/cm^2 [26, 27], suggesting that VEGF may be superior to antibodies in capturing cells under physiological conditions. One possible explanation may be because the dissociation constant of the anti-VEGFR2:VEGFR2 interaction is ~1,000 fold higher than that of VEGF:VEGFR2 (anti-VEGFR2:VEGFR2, $K_D=6.9\times10^{-9}$ M; as opposed to VEGF:VEGFR2, $K_D=14–51\times10^{-12}$ M) indicating that the binding affinity of receptor/ligand is much higher than that of receptor/antibody [26, 85, 86]. It is important to note that in our experiments, cell number and density was standardized, and therefore, the time that each sample spent in the device varied from 45 min at low shear to 2.2 min at high shear stress. This suggests that if the time of each run were kept constant by running larger volumes at high shear stress, the number of cells would increase significantly. Indeed, when the running time of high shear runs increased from 2.2 min to 45 min (same as the time of low shear runs) the number of captured cells increased nearly four times (from 66 to 237 cells/mm^2) (Fig. S2).

VEGF mediated capture was highly selective. Endothelial cells, as represented by HUVECs and OPAECs showed similar capture rates, whereas non-EC represented by hHF-MSC, h-dFB, and NIH-3T3 did not bind to an extent that was statistically significant as compared to control conditions (no VEGF). In contrast, antibody-mediated capture resulted in low but significant capture of non-endothelial cells [26]. Considering the highly selective nature of VEGF towards EC, we hypothesized that cell capture might be dependent on activation of the high affinity VEGF receptor, VEGFR2 or KDR [87–89]. Indeed, inhibiting VEGFR2 using SU5416 [78], a well-known and potent chemical inhibitor of VEGFR2 function, completely inhibited VEGF-mediated EC capture. Therefore, it is reasonable to conclude that receptor355 mediated binding and signaling is necessary for yielding highly selective EC capture.

We can reasonably conclude that the cell capture observed was driven only by VEGF:VEGFR binding as shown by the following evidence: (i) lack of capture observed when treating the cells with SU5416; (ii) insignificant capture observed when the surface was coated with heparin but without VEGF; and (iii) no significant capture above control conditions was observed for non-EC cells i.e. NIH-3T3s, h-DFBs, and hHF-MSCs, which do not express functional VEGF receptors. Control surfaces contained heparin but were devoid of VEGF and failed to any capture EC at any shear stress in the range tested (Fig. 4B). They also did not capture any non-EC cells (Fig. 5A). Removal of heparin left the surface coated with poly-L-lysine, which was not permissive to VEGF binding as shown in Fig. 1C. In our studies, we used EDTA to detach the cells from the surface in order to preserve the function of surface receptors, including the VEGFRs. This likely preserved surface-associated ECM molecules, which could assist in VEGF mediated capture. However, omission of serum in all flow experiments mitigated any effect that serum proteins, e.g. fibronectin, might have had on capture through cell surface receptors other than VEGFR, e.g. integrins. In addition, all non-EC cells were also lifted with EDTA but capture was insignificant. Taken together, our results suggest that a functional VEGF receptor was crucial for successful EC capture under flow.

In addition to capturing EC from homogenous cell solutions, immobilized VEGF could capture EC from mixtures with non-EC, such as NIH-3T3 at varying ratios. As expected, the efficiency of VEGF-mediated EC capture decreased at high shear stress. However, for the same shear stress, the percentage of captured cells was independent of the ratio of EC to non-EC cells (1:100 or $1:10^6$), suggesting that cell capture efficiency depended primarily on the concentration of EC but was independent of the presence of other cells that did not compete for binding to VEGF. Notably, VEGF could capture pre-labeled EC that were spiked into whole blood at very low ratio ($1:10^6$ EC; 5×10^3 EC were added into 1 mL of blood containing 5×10^9 cells [90]). This result may have far reaching implications, as it suggests that VEGF could be used to promote endothelialization of vascular grafts or neovascularization of implanted tissues by rare but continuously circulating EPCs. We are currently working to address this interesting hypothesis.

Conclusions

In conclusion, we demonstrated that immobilized human VEGF-165 could capture EC under low or high shear stress with high selectivity. Cell binding to immobilized VEGF activated VEGFR2, which was necessary for capture. VEGFR2 activation increased proliferation of captured EC, demonstrating that VEGF might be useful in promoting endothelialization of vascular grafts or neovascularization of implants.

Supplementary Material

Refer to Web version on PubMed Central for supplementary material.

Acknowledgements

This work was supported by a grant from the National Heart and Lung Institute (R01 HL086582) to S.T.A. and D.D.S.

References

1. Lloyd-Jones D, Adams RJ, Brown TM, Carnethon M, Dai S, De Simone G, et al. Heart disease and stroke statistics--2010 update: a report from the American Heart Association. Circulation. 2010; 121:e46–e215. [PubMed: 20019324]
2. Seifalian AM, Tiwari A, Hamilton G, Salacinski HJ. Improving the clinical patency of prosthetic vascular and coronary bypass grafts: the role of seeding and tissue engineering. Artif Organs. 2002; 26:307–320. [PubMed: 11952502]
3. Veith FJ, Moss CM, Sprayregen S, Montefusco C. Preoperative saphenous venography in arterial reconstructive surgery of the lower extremity. Surgery. 1979; 85:253–256. [PubMed: 424995]
4. Gaudino M, Cellini C, Pragliola C, Trani C, Burzotta F, Schiavoni G, et al. Arterial versus venous bypass grafts in patients with in-stent restenosis. Circulation. 2005; 112:I265–I269. [PubMed: 16159829]
5. Gao J, Niklason L, Langer R. Surface hydrolysis of poly(glycolic acid) meshes increases the seeding density of vascular smooth muscle cells. J Biomed Mater Res. 1998; 42:417–424. [PubMed: 9788505]
6. Gong Z, Niklason LE. Blood vessels engineered from human cells. Trends Cardiovasc Med. 2006; 16:153–156. [PubMed: 16781948]

7. Gong Z, Niklason LE. Small-diameter human vessel wall engineered from bone marrow-derived mesenchymal stem cells (hMSCs). FASEB journal : official publication of the Federation of American Societies for Experimental Biology. 2008; 22:1635–1648. [PubMed: 18199698]
8. Huang AH, Niklason LE. Engineering biological-based vascular grafts using a pulsatile bioreactor. J Vis Exp. 2011
9. McKee JA, Banik SS, Boyer MJ, Hamad NM, Lawson JH, Niklason LE, et al. Human arteries engineered in vitro. EMBO Rep. 2003; 4:633–638. [PubMed: 12776184]
10. Niklason LE, Gao J, Abbott WM, Hirschi KK, Houser S, Marini R, et al. Functional arteries grown in vitro. Science. 1999; 284:489–493. [PubMed: 10205057]
11. Poh M, Boyer M, Solan A, Dahl SL, Pedrotty D, Banik SS, et al. Blood vessels engineered from human cells. Lancet. 2005; 365:2122–2124. [PubMed: 15964449]
12. Prabhakar V, Grinstaff MW, Alarcon J, Knors C, Solan AK, Niklason LE. Engineering porcine arteries: effects of scaffold modification. Journal of biomedical materials research Part A. 2003; 67:303–311. [PubMed: 14517890]
13. L'Heureux N, Dusserre N, Konig G, Victor B, Keire P, Wight TN, et al. Human tissue-engineered blood vessels for adult arterial revascularization. Nat Med. 2006; 12:361–365. [PubMed: 16491087]
14. L'Heureux N, Dusserre N, Marini A, Garrido S, de la Fuente L, McAllister T. Technology insight: the evolution of tissue-engineered vascular grafts--from research to clinical practice. Nat Clin Pract Cardiovasc Med. 2007; 4:389–395. [PubMed: 17589429]
15. L'Heureux N, Germain L, Labbe R, Auger FA. In vitro construction of a human blood vessel from cultured vascular cells: a morphologic study. Journal of vascular surgery. 1993; 17:499–509. [PubMed: 8445745]
16. L'Heureux N, McAllister TN, de la Fuente LM. Tissue-engineered blood vessel for adult arterial revascularization. N Engl J Med. 2007; 357:1451–1453. [PubMed: 17914054]
17. L'Heureux N, Paquet S, Labbe R, Germain L, Auger FA. A completely biological tissue-engineered human blood vessel. FASEB journal : official publication of the Federation of American Societies for Experimental Biology. 1998; 12:47–56. [PubMed: 9438410]
18. Quint C, Arief M, Muto A, Dardik A, Niklason LE. Allogeneic human tissue-engineered blood vessel. Journal of vascular surgery. 2011
19. Dahl SL, Kypson AP, Lawson JH, Blum JL, Strader JT, Li Y, et al. Readily available tissue-engineered vascular grafts. Sci Transl Med. 2011; 3:68ra9.
20. Syedain ZH, Meier LA, Lahti MT, Johnson SL, Tranquillo RT. Implantation of completely biological engineered grafts following decellularization into the sheep femoral artery. Tissue engineering Part A. 2014; 20:1726–1734. [PubMed: 24417686]
21. Wystrychowski W, McAllister TN, Zagalski K, Dusserre N, Cierpka L, L'Heureux N. First human use of an allogeneic tissue-engineered vascular graft for hemodialysis access. Journal of vascular surgery. 2013
22. Peng H, Schlaich EM, Row S, Andreadis ST, Swartz DD. A novel ovine ex vivo arteriovenous shunt model to test vascular implantability. Cells, tissues, organs. 2012; 195:108–121. [PubMed: 22005667]
23. Wu W, Allen RA, Wang Y. Fast-degrading elastomer enables rapid remodeling of a cell-free synthetic graft into a neoartery. Nat Med. 2012; 18:1148–1153. [PubMed: 22729285]
24. Pratt ED, Huang C, Hawkins BG, Gleghorn JP, Kirby BJ. Rare cell capture in microfluidic devices. Chemical Engineering Science. 2011; 66:1508–1522. [PubMed: 21532971]
25. Angelos MG, Brown MA, Satterwhite LL, Levering VW, Shaked NT, Truskey GA. Dynamic Adhesion of Umbilical Cord Blood Endothelial Progenitor Cells under Laminar Shear Stress. Biophysical Journal. 2010; 99:3545–3554. [PubMed: 21112278]
26. Plouffe BD, Kniazeva T, Mayer JE Jr, Murthy SK, Sales VL. Development of microfluidics as endothelial progenitor cell capture technology for cardiovascular tissue engineering and diagnostic medicine. FASEB journal : official publication of the Federation of American Societies for Experimental Biology. 2009; 23:3309–3314. [PubMed: 19487310]

27. Markway BD, McCarty OJT, Marzec UM, Courtman DW, Hanson SR, Hinds MT. Capture of flowing endothelial cells using surface-immobilized anti-kinase insert domain receptor antibody. Tissue 458 engineering Part C, Methods. 2008; 14:97–105.

28. Irace C, Carallo C, De Franceschi MS, Scicchitano F, Milano M, Tripolino C, et al. Human common carotid wall shear stress as a function of age and gender: a 12-year follow-up study. Age. 2012; 34:1553–1562. [PubMed: 21989971]

29. Anderson SM, Chen TT, Iruela-Arispe ML, Segura T. The phosphorylation of vascular endothelial growth factor receptor-2 (VEGFR-2) by engineered surfaces with electrostatically or covalently immobilized VEGF. Biomaterials. 2009; 30:4618–4628. [PubMed: 19540581]

30. Chen TT, Luque A, Lee S, Anderson SM, Segura T, Iruela-Arispe ML. Anchorage of VEGF to the extracellular matrix conveys differential signaling responses to endothelial cells. The Journal of cell biology. 2010; 188:595–609. [PubMed: 20176926]

31. Fan VH, Tamama K, Au A, Littrell R, Richardson LB, Wright JW, et al. Tethered epidermal growth factor provides a survival advantage to mesenchymal stem cells. Stem cells (Dayton, Ohio). 2007; 25:1241–1251.

32. Leclerc C, Brose C, Nouze C, Leonard F, Majlessi L, Becker S, et al. Immobilized cytokines as biomaterials for manufacturing immune cell based vaccines. Journal of biomedical materials research Part A. 2008; 86:1033–1040. [PubMed: 18067172]

33. Mann BK, Schmedlen RH, West JL. Tethered-TGF-beta increases extracellular matrix production of vascular smooth muscle cells. Biomaterials. 2001; 22:439–444. [PubMed: 11214754]

34. Platt MO, Roman AJ, Wells A, Lauffenburger DA, Griffith LG. Sustained epidermal growth factor receptor levels and activation by tethered ligand binding enhances osteogenic differentiation of multi-potent marrow stromal cells. Journal of cellular physiology. 2009; 221:306–317. [PubMed: 19544388]

35. Yu LM, Wosnick JH, Shoichet MS. Miniaturized system of neurotrophin patterning for guided regeneration. Journal of neuroscience methods. 2008; 171:253–263. [PubMed: 18486231]

36. Zisch AH, Schenk U, Schense JC, Sakiyama-Elbert SE, Hubbell JA. Covalently conjugated VEGF--fibrin matrices for endothelialization. Journal of controlled release : official journal of the Controlled Release Society. 2001; 72:101–113. [PubMed: 11389989]

37. Geer DJ, Swartz DD, Andreadis ST. Biomimetic delivery of keratinocyte growth factor upon cellular demand for accelerated wound healing in vitro and in vivo. The American journal of pathology. 2005; 167:1575–1586. [PubMed: 16314471]

38. Hu X, Neoh KG, Zhang J, Kang ET, Wang W. Immobilization strategy for optimizing VEGF's concurrent bioactivity towards endothelial cells and osteoblasts on implant surfaces. Biomaterials. 2012; 33:8082–8093. [PubMed: 22884814]

39. Sasaki M, Inoue M, Katada Y, Taguchi T. The effect of VEGF-immobilized nickel-free high-nitrogen stainless steel on viability and proliferation of vascular endothelial cells. Colloids and Surfaces B: Biointerfaces. 2012; 92:1–8.

40. Liang MS, Andreadis ST. Engineering fibrin-binding TGF-beta1 for sustained signaling and contractile function of MSC based vascular constructs. Biomaterials. 2011; 32:8684–8693. [PubMed: 21864893]

41. Wijelath ES, Rahman S, Namekata M, Murray J, Nishimura T, Mostafavi-Pour Z, et al. Heparin-II domain of fibronectin is a vascular endothelial growth factor-binding domain: enhancement of VEGF biological activity by a singular growth factor/matrix protein synergism. Circulation research. 2006; 99:853–860. [PubMed: 17008606]

42. Benoit DS, Anseth KS. Heparin functionalized PEG gels that modulate protein adsorption for hMSC adhesion and differentiation. Acta biomaterialia. 2005; 1:461–470. [PubMed: 16701827]

43. Schroeder-Tefft JA, Bentz H, Estridge TD. Collagen and heparin matrices for growth factor delivery. Journal of Controlled Release. 1997; 49:291–298.

44. Yamaguchi N, Kiick KL. Polysaccharide-poly(ethylene glycol) star copolymer as a scaffold for the production of bioactive hydrogels. Biomacromolecules. 2005; 6:1921–1930. [PubMed: 16004429]

45. Maharaj ASR, D'Amore PA. Roles for VEGF in the adult. Microvascular Research. 2007; 74:100–113. [PubMed: 17532010]

46. Ho QT, Kuo CJ. Vascular endothelial growth factor: Biology and therapeutic applications. The International Journal of Biochemistry & Cell Biology. 2007; 39:1349–1357. [PubMed: 17537667]
47. Otrock ZK, Makarem JA, Shamseddine AI. Vascular endothelial growth factor family of ligands and receptors: Review. Blood Cells, Molecules, and Diseases. 2007; 38:258–268.
48. Ng Y-S, Krilleke D, Shima DT. VEGF function in vascular pathogenesis. Experimental Cell Research. 2006; 312:527–537. [PubMed: 16330026]
49. Li X, Eriksson U. Novel VEGF family members: VEGF-B, VEGF-C and VEGF-D. The International Journal of Biochemistry & Cell Biology. 2001; 33:421–426. [PubMed: 11312110]
50. Ferrara N. The Biology of Vascular Endothelial Growth Factor. Endocrine Reviews. 1997; 18:4–25. [PubMed: 9034784]
51. Klagsbrun M, A D'Amore P. Vascular endothelial growth factor and its receptors. Cytokine & Growth Factor Reviews. 1996; 7:259–270. [PubMed: 8971481]
52. Klagsbrun M, Soker S. VEGF/VPF: The angiogenesis factor found? 1993:699–702.
53. Park JE, Keller GA, Ferrara N. The vascular endothelial growth factor (VEGF) isoforms: differential deposition into the subepithelial extracellular matrix and bioactivity of extracellular matrix-bound VEGF. Molecular biology of the cell. 1993; 4:1317–1326. [PubMed: 8167412]
54. Terman BI, Dougher-Vermazen M, Carrion ME, Dimitrov D, Armellino DC, Gospodarowicz D, et al. Identification of the KDR tyrosine kinase as a receptor for vascular endothelial cell growth factor. Biochemical and biophysical research communications. 1992; 187:1579–1586. [PubMed: 1417831]
55. Tischer E, Gospodarowicz D, Mitchell R, Silva M, Schilling J, Lau K, et al. Vascular endothelial growth factor: A new member of the platelet-derived growth factor gene family. Biochemical and Biophysical Research Communications. 1989; 165:1198–1206. [PubMed: 2610687]
56. Bikfalvi A, Bicknell R. Recent advances in angiogenesis, anti-angiogenesis and vascular targeting. Trends in Pharmacological Sciences. 2002; 23:576–582. [PubMed: 12457776]
57. Ferrara N. VEGF: an update on biological and therapeutic aspects. Current Opinion in Biotechnology. 2000; 11:617–624. [PubMed: 11102799]
58. Ferrara N. Role of vascular endothelial growth factor in the regulation of angiogenesis. Kidney international. 1999; 56:794–814. [PubMed: 10469350]
59. Korpelainen EI, Alitalo K. Signaling angiogenesis and lymphangiogenesis. Current Opinion in Cell Biology. 1998; 10:159–164. [PubMed: 9561839]
60. Risau W. Mechanisms of angiogenesis. Nature. 1997; 386:671–674. [PubMed: 9109485]
61. Keck PJ, Hauser SD, Krivi G, Sanzo K, Warren T, Feder J, et al. Vascular permeability factor, an endothelial cell mitogen related to PDGF. Science (New York, NY). 1989; 246:1309–1312.
62. Folkman J, Klagsbrun M. Angiogenic factors. Science (New York, NY). 1987; 235:442–447.
63. Keyt BA, Berleau LT, Nguyen HV, Chen H, Heinsohn H, Vandlen R, et al. The carboxyl-terminal domain (111–165) of vascular endothelial growth factor is critical for its mitogenic potency. The Journal of biological chemistry. 1996; 271:7788–7795. [PubMed: 8631822]
64. Gitay-Goren H, Soker S, Vlodavsky I, Neufeld G. The binding of vascular endothelial growth factor to its receptors is dependent on cell surface-associated heparin-like molecules. The Journal of biological chemistry. 1992; 267:6093–6098. [PubMed: 1556117]
65. Nakamura S, Kubo T, Ijima H. Heparin-conjugated gelatin as a growth factor immobilization scaffold. Journal of Bioscience and Bioengineering. 2013; 115:562–567. [PubMed: 23273911]
66. Sharon JL, Puleo DA. Immobilization of glycoproteins, such as VEGF, on biodegradable substrates. Acta Biomaterialia. 2008; 4:1016–1023. [PubMed: 18359670]
67. Maile LA, Busby WH, Sitko K, Capps BE, Sergent T, Badley-Clarke J, et al. The heparin binding domain of vitronectin is the region that is required to enhance insulin-like growth factor-I signaling. Molecular endocrinology (Baltimore, Md). 2006; 20:881–892.
68. Mitsi M, Hong Z, Costello CE, Nugent MA. Heparin-mediated conformational changes in fibronectin expose vascular endothelial growth factor binding sites. Biochemistry. 2006; 45:10319–10328. [PubMed: 16922507]

69. Ricard-Blum S, Beraud M, Raynal N, Farndale RW, Ruggiero F. Structural requirements for heparin/heparan sulfate binding to type V collagen. The Journal of biological chemistry. 2006; 281:25195–25204. [PubMed: 16815843]
70. Wijelath ES, Murray J, Rahman S, Patel Y, Ishida A, Strand K, et al. Novel vascular endothelial growth factor binding domains of fibronectin enhance vascular endothelial growth factor biological activity. Circulation research. 2002; 91:25–31. [PubMed: 12114318]
71. Yamashita H, Beck K, Kitagawa Y. Heparin binds to the laminin alpha4 chain LG4 domain at a site different from that found for other laminins. Journal of molecular biology. 2004; 335:1145–1149. [PubMed: 14729333]
72. Liu JY, Peng HF, Andreadis ST. Contractile smooth muscle cells derived from hair-follicle stem cells. Cardiovasc Res. 2008; 79:24–33. [PubMed: 18316325]
73. Swartz DD, Russell JA, Andreadis ST. Engineering of fibrin-based functional and implantable small-diameter blood vessels. American journal of physiology Heart and circulatory physiology. 2005; 288:H1451–H1460. [PubMed: 15486037]
74. Smith PK, Mallia AK, Hermanson GT. Colorimetric method for the assay of heparin content in immobilized heparin preparations. Analytical biochemistry. 1980; 109:466–473. [PubMed: 7224172]
75. Fröhlich E, Bonstingl G, Höfler A, Meindl C, Leitinger G, Pieber TR, et al. Comparison of two in vitro systems to assess cellular effects of nanoparticles-containing aerosols. Toxicology in Vitro. 2013; 27–360:409–417.
76. Barrantes A, Santos O, Sotres J, Arnebrant T. Influence of pH on the build-up of poly-L-lysine/heparin multilayers. Journal of colloid and interface science. 2012; 388:191–200. [PubMed: 22958851]
77. Dayanir V, Meyer RD, Lashkari K, Rahimi N. Identification of tyrosine residues in vascular endothelial growth factor receptor-2/FLK-1 involved in activation of phosphatidylinositol 3-kinase and cell proliferation. The Journal of biological chemistry. 2001; 276:17686–17692. [PubMed: 11278468]
78. Fong TAT, Shawver LK, Sun L, Tang C, App H, Powell TJ, et al. SU5416 Is a Potent and Selective Inhibitor of the Vascular Endothelial Growth Factor Receptor (Flk-1/KDR) That Inhibits Tyrosine Kinase Catalysis, Tumor Vascularization, and Growth of Multiple Tumor Types. Cancer Research. 1999; 59:99–106. [PubMed: 9892193]
79. Kim S, von Recum H. Endothelial stem cells and precursors for tissue engineering: cell source, differentiation, selection, and application. Tissue Eng Part B Rev. 2008; 14:133–147. [PubMed: 18454639]
80. DeLong SA, Moon JJ, West JL. Covalently immobilized gradients of bFGF on hydrogel scaffolds for directed cell migration. Biomaterials. 2005; 26:3227–3234. [PubMed: 15603817]
81. Gobin AS, West JL. Effects of epidermal growth factor on fibroblast migration through biomimetic hydrogels. Biotechnology progress. 2003; 19:1781–1785. [PubMed: 14656156]
82. Gobin AS, West JL. Cell migration through defined, synthetic ECM analogs. FASEB journal : official publication of the Federation of American Societies for Experimental Biology. 2002; 16:751–753. Epub 2002 Mar 26. [PubMed: 11923220]
83. Yu J, Wang A, Tang Z, Henry J, Li-Ping Lee B, Zhu Y, et al. The effect of stromal cell-derived factor-1alpha/heparin coating of biodegradable vascular grafts on the recruitment of both endothelial and smooth muscle progenitor cells for accelerated regeneration. Biomaterials. 2012; 33:8062–8074. [PubMed: 22884813]
84. Lee KW, Johnson NR, Gao J, Wang Y. Human progenitor cell recruitment via SDF-1alpha coacervate-laden PGS vascular grafts. Biomaterials. 2013; 34:9877–9885. [PubMed: 24060423]
85. Huang J, Tan Y, Tang Q, Liu X, Guan X, Feng Z, et al. A high-affinity human/mouse cross-reactive monoclonal antibody, specific for VEGFR-2 linear and conformational epitopes. Cytotechnology. 2010; 62:61–71. [PubMed: 20387114]
86. Cunningham SA, Tran TM, Arrate MP, Brock TA. Characterization of vascular endothelial cell growth factor interactions with the kinase insert domain-containing receptor tyrosine kinase. A real time kinetic study. The Journal of biological chemistry. 1999; 274:18421–18427. [PubMed: 10373449]

87. Nakayama M, Berger P. Coordination of VEGF receptor trafficking and signaling by coreceptors. Experimental Cell Research. 2013; 319:1340–1347. [PubMed: 23499743]

88. Eichmann A, Simons M. VEGF signaling inside vascular endothelial cells and beyond. Current Opinion in Cell Biology. 2012; 24:188–193. [PubMed: 22366328]

89. Koch S, Tugues S, Li X, Gualandi L, Claesson-Welsh L. Signal transduction by vascular endothelial growth factor receptors. The Biochemical journal. 2011; 437:169–183. [PubMed: 21711246]

90. Suzuki Y, Yamamoto K, Ando J, Matsumoto K, Matsuda T. Arterial shear stress augments the differentiation of endothelial progenitor cells adhered to VEGF-bound surfaces. Biochemical and Biophysical Research Communications. 2012; 423:91–97. [PubMed: 22634005]

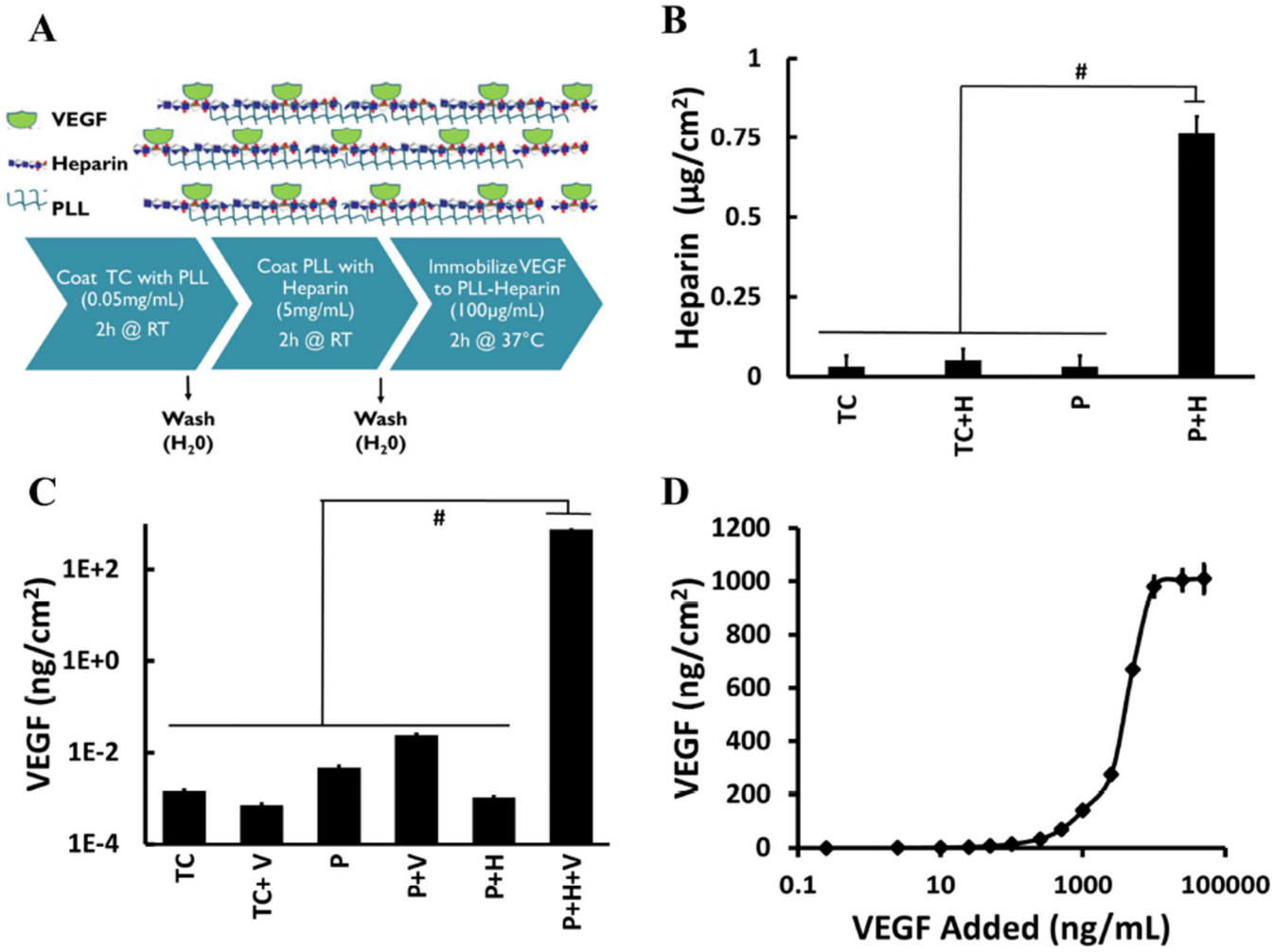

Figure 1. Assembly of modified surface for VEGF immobilization

(A) Schematic of the modified surface with immobilized VEGF. **(B)** Heparin binds to PLL but not to TC plates. The concentration of heparin bound to PLL was determined by toluidine blue binding and subsequent absorbance reading. **(C)** VEGF surface concentration of PLL-bound heparin; y-axis in logarithmic scale. **(D)** Immobilized VEGF surface concentration (ng/cm^2) as a function of input VEGF concentration in solution (ng/mL). Approximately ~64% of VEGF bound to heparin when the concentration of input VEGF was in the range between 100ng and 1000ng/well; x-axis is in logarithmic scale. (#) denotes statistical significance ($p<0.05$, $n=3$) between the indicated samples. Legend: TC: Tissue culture treated plate with no heparin or PLL; TC+H: tissue culture treated plate incubated with heparin; P: Surface treated (TC) with PLL and no heparin or VEGF; P+H: Surface treated with PLL and Heparin; TC+V: surface treated with VEGF alone; P+V: surface treated with PLL then VEGF; P+H+V: surface treated with PLL then heparin and then VEGF.

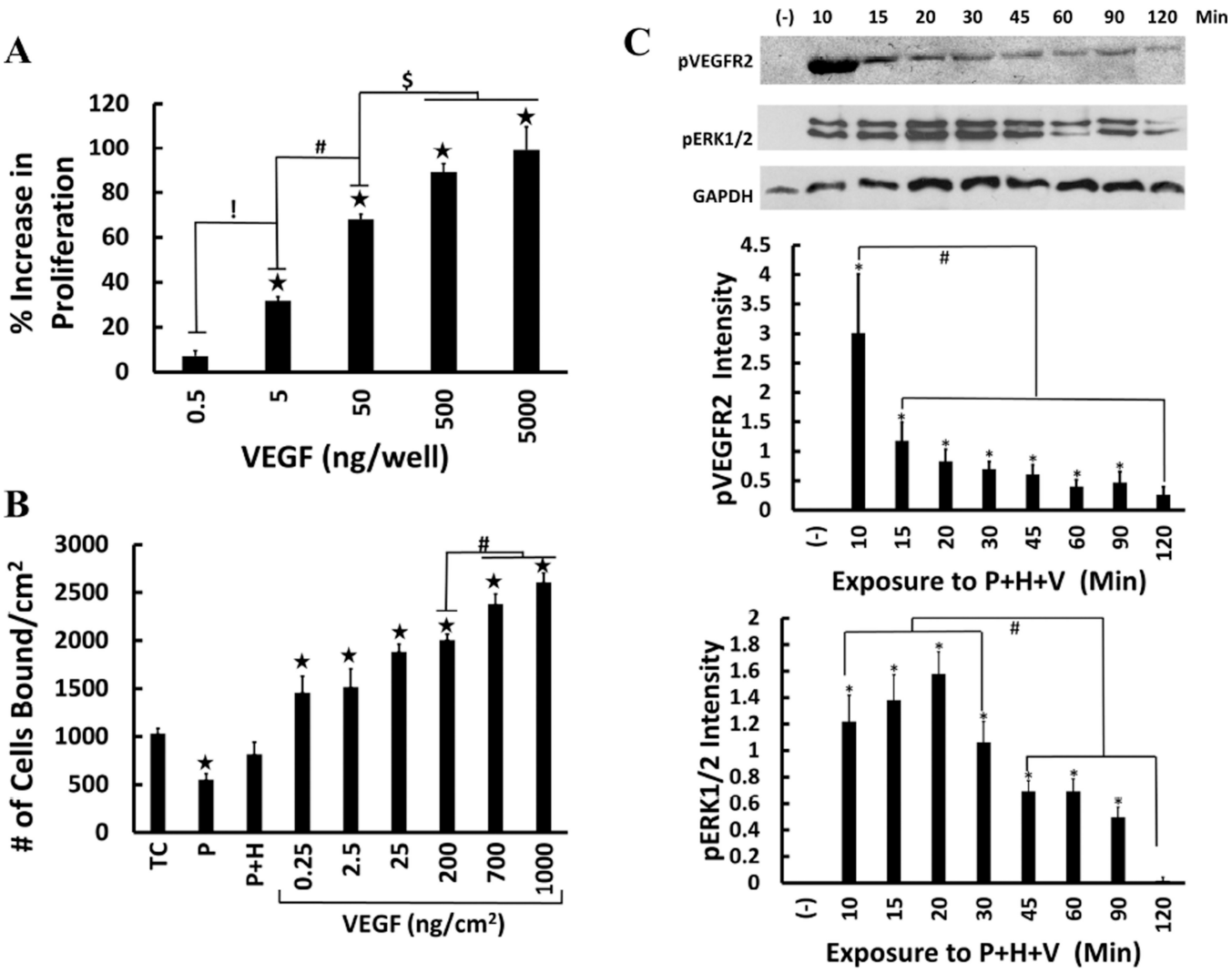

Figure 2. HUVEC capture and proliferation on VEGF-functionalized surfaces

(A) Proliferation of HUVECs cultured on VEGF surface. Cells were seeded (5×10^3 cells/well of 48 well plate) in basal EBM2 with 10% serum for 6 hr to allow proper spreading before changing the media to a basal media (M199) with 2% serum and allowed to grow for a period of 5 days. Proliferation was measured using the MTT assay and reported as % increase as compared to the P+H surface. **(B)** Capture of HUVECs as a function of immobilized VEGF surface concentration. Briefly HUVECs (5×10^3 cells/well of 48 well plate) were plated onto VEGF functionalized surface for 30 min in the absence of serum. At that time, unbound cells were washed with PBS and the remaining cells were fixed, stained with DAPI and counted. (★) denotes statistical significance ($p<0.05$, n=3) between the P+H+V and P+H surfaces, ($, #, !) denotes statistical significance ($p<0.05$, n=3) between the two data points. **(C)** Western Blot for pVEGFR2 and its downstream effector pERK1/2. HUVEC were allowed to bind to immobilized VEGF for the indicated times prior to lysis. Bar Graphs; quantification (densitometry) of western blot bands (n=3), normalized values to GAPDH. GAPDH served as loading control. (*) denotes statistical significance ($p<0.05$, n=3) between the P+H+V and P+H surfaces, (#) denotes statistical significance ($p<0.05$,

n=3) between the indicated time points. Legend: P+H+V: surface treated with PLL then heparin then VEGF; P+H: surface treated with PLL then heparin (no VEGF) served as negative control.

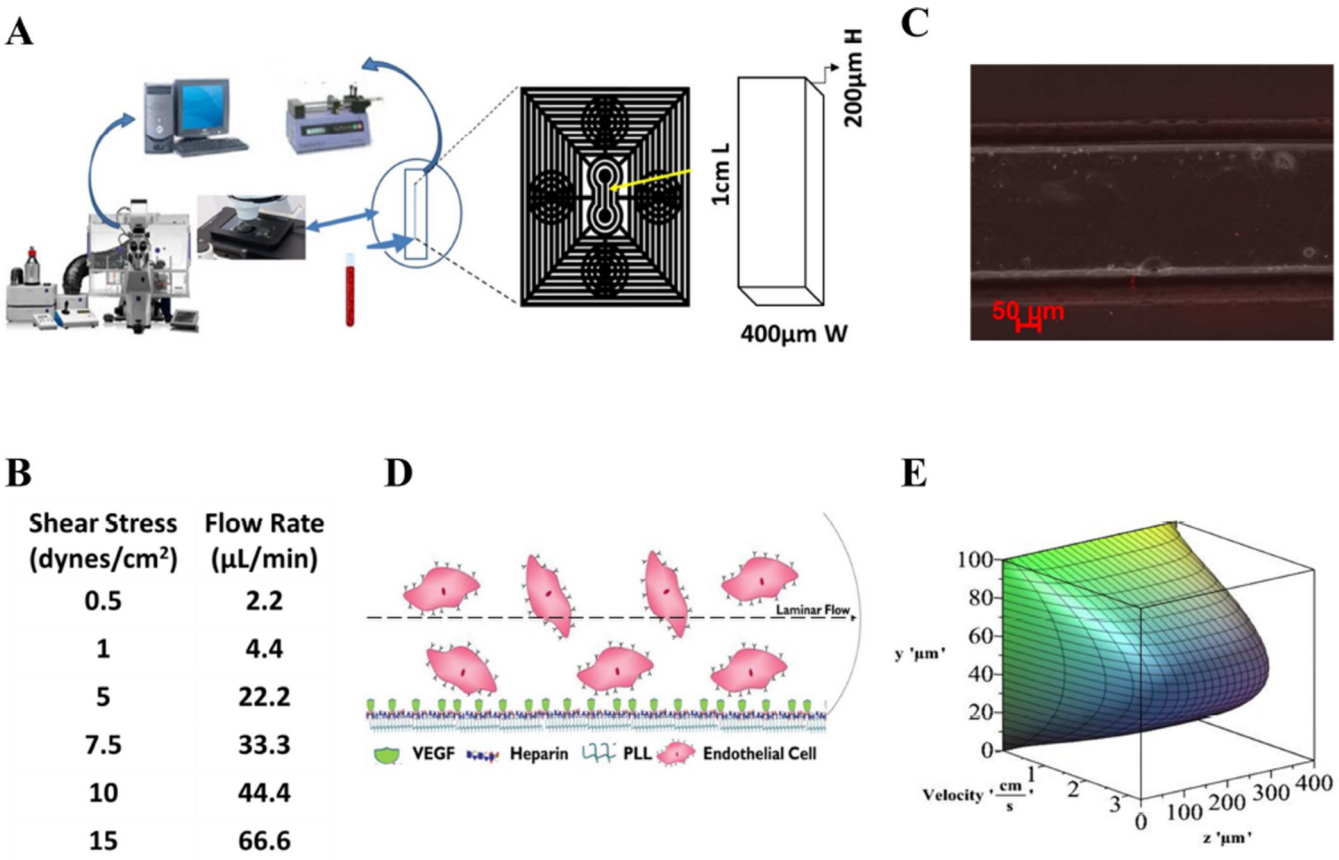

Figure 3. Microfluidic device for capture of cells under shear

(A) Schematic of vacuum-sealed fluidic device and setup within a Zeiss fluorescence microscope containing an incubator chamber with temperature and CO_2 controlled environment. The channel has dimensions of 200µm height (H), 400 µm width (W), and 1cm length (L). **(B)** Calculated shear stress on the surface for the indicated flow rates. **(C)** Image of fluidic channel within the fluidic device. **(D)** Schematic of EC capture on the micro-channel. **(E)** The laminar flow profile in microfluidic channel was derived analytically from the Navier-Stokes equations for rectangular geometry, considering zero velocity at the walls, as boundary conditions. The parabolic flow profile was plotted using Maple (Version 17).

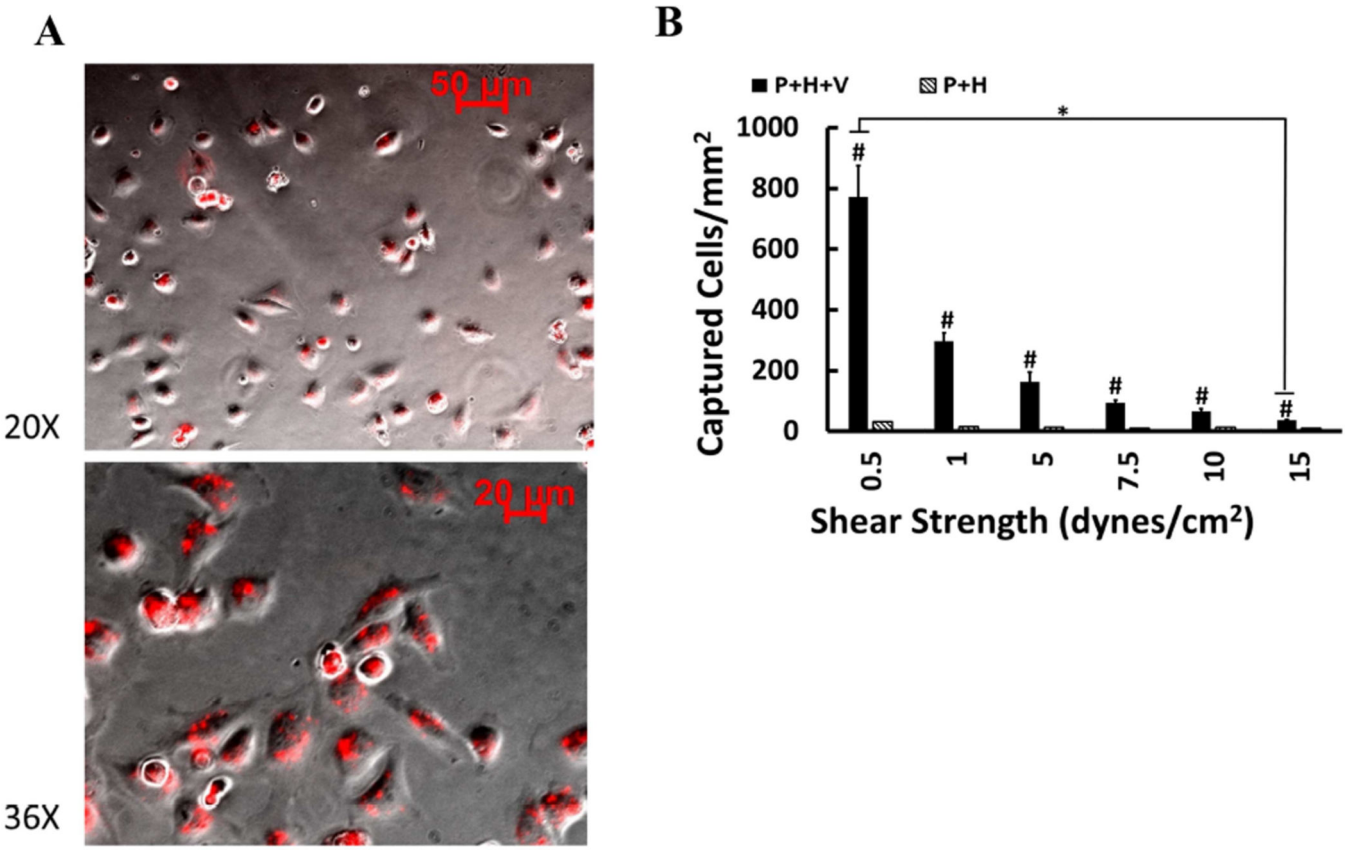

Figure 4. Capture of HUVEC under shear

(A) Representative image of HUVECs captured on VEGF functionalized surface under low shear stress (0.5 dyne/cm^2) at two magnifications (20× and 36×). Captured cells spread within 20 min and were stained with membrane tracker DIL (red). The picture is an overlay of fluorescence and brightfield images. **(B)** Capture of HUVECs on VEGF functionalized surface as a function of shear stress. HUVECs were pretreated with membrane dye DIL (red fluorescence), detached from the surface with 5mM EDTA solution and passed through the micro-channel at various flow rates. Each "run" is defined as 100 μL of sample containing 10,000 cells. Total time for each run varied with shear stress, from 86 s at high shear (15 dyne/cm^2) to 45 min at low shear (0.5 dyne/cm^2). (#) denotes statistical significance ($p<0.05$, n=3 for shear stress between 0.5–7.5 dyne/cm^2; n=10 for shear stress between 10–15 dyne/cm^2) between P+H+V and P+H surfaces. Legend: P+H+V: surface treated with PLL then heparin then VEGF; P+H: surface treated with PLL then heparin (no VEGF) served as negative control.

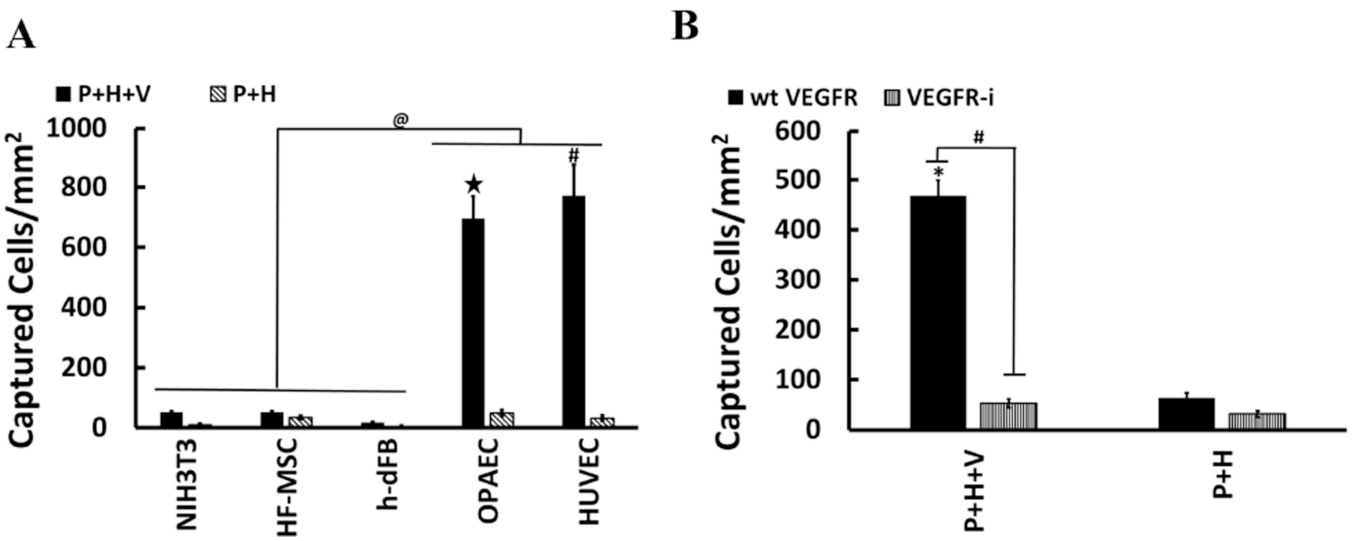

Figure 5. VEGF captures Endothelial Cells with high specificity

(A) Two types of endothelial cells, HUVECs and Ovine Pulmonary Artery Endothelial cells (OPAECs) and three non-EC, HF-MSC, NIH-3T3 and h-dFB were tested at low shear (0.5 dyne/cm^2). Only EC bound to VEGF functionalized surface. **(B)** HUVECs were treated SU5416 (1 μM for 60 min then media was replaced with fresh media O/N to achieve cellular quiescence) prior to flow over VEGF functionalized surface. (#) denotes statistical significance ($p<0.05$, $n=3$) between the control and SU5416 treated samples. Legend: P+H +V: surface treated with PLL then heparin then VEGF; P+H: surface treated with PLL then heparin (no VEGF) served as negative control.

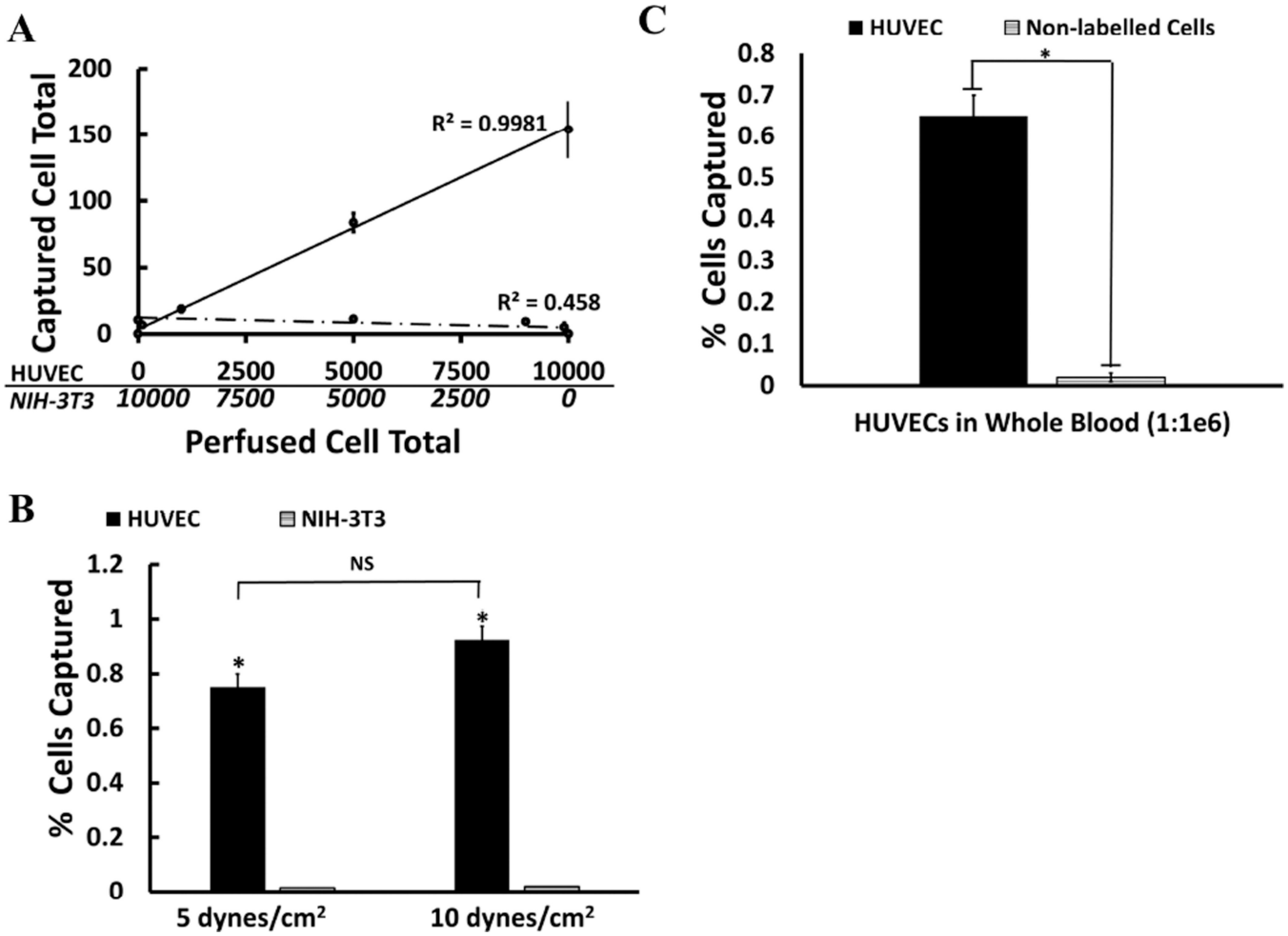

Figure 6. HUVEC capture from complex cell mixtures

(A) Capture of EC at low shear (0.5 dyne/cm^2) from dual cell mixtures of HUVECs and NIH-3T3 cells of 1:0, 0:1, 1:1, 1:10, or 1:100 ratio. HUVECs and NIH-3T3 were pre-labeled with DIL and DIO, respectively prior to running through the fluidic device. The solid line indicates captured HUVECs and the dotted line captured NIH-3T3 cells. **(B)** EC capture from a HUVEC:NIH-3T3 mixture (ratio 1:100) under intermediate (5 dyne/cm^2) or high shear stress (10 dyne/cm^2). **(C)** HUVEC were pre-labeled with DII and spiked into whole human blood at 5×10^3 cells per mL of blood (HUVEC: Blood cell ratio=10^6). Then 1mL of HUVEC containing blood was passed through the micro-channel at high shear stress (10 dyne/cm^2). (*) denotes statistical significance ($p<0.05$, n=5) above the indicated samples.